Engineering and Technology Journal
Journal homepage: https://etj.uotechnology.edu.iq

Numerical Simulation of Powering Turbofan Propulsion Aircraft with Electricity

Thomas O. Onah[*a], **Christian C. Aka**[a], **Bertrand N. Nwankwojike**[b]

[a] Mechanical and Production Engineering, Enugu State University of Science and Technology, Enugu, Nigeria.
[b] Mechanical Engineering, Michael Okpara University of Agriculture, Umudike, Nigeria
*Corresponding author Email: okechukwutm@yahoo.com

HIGHLIGHTS

- This research is focused on the propulsion of aircraft using electricity.
- More electric aircraft approach has allowed the older power subsystems to be replaced by electrical systems within modern aircraft.
- The result of the lift power requirement should be a boost for battery companies to develop FWA.
- The result of the current study inferred that the Flying Wing Aircraft is more aerodynamic and would improve aircraft efficiency and emit less emission.

ARTICLE INFO

Handling editor: Sattar. Aljabair

Keywords:
Turbofan; Electricity-aircraft; Convectional-aircraft; Computational- Fluid-Dynamics; Forces.

ABSTRACT

The gas turbine-based propulsion systems were responsible for the emission of pollutants that damage the ecosphere. Commercial aviation represented a large portion of carbon emissions within the aviation industry, so this study focused on novel aircraft propulsion systems for large commercial aircraft. Electric propulsion was considered to be an alternative to conventional propulsion systems. Therefore, this report analyzed the various electric aircraft concepts within the aerospace industry to see whether they have environmental benefits. A flying wing aircraft was compared to a conventional tube-and-wing aircraft using Computational Fluid Dynamics to determine which aircraft requires more power. The lift forces acting on the conventional aircraft and flying wing at cruise speed were 269,110 N and 10681 N, while the drag forces acting on the conventional aircraft and Flying Wing Aircraft at cruise speed were 260,940N and 7679N, respectively. More electric aircraft approach has allowed the older power subsystems to be replaced by electrical systems within modern aircrafts such as the Boeings, airbus, etc. This has increased fuel efficiency. The result of the lift power requirement should be a boost for battery companies to develop FWA. Conclusively, the result inferred that the Flying Wing Aircraft is more aerodynamic and, therefore, would improve aircraft efficiency and emit less emission.

1. Introduction

The Air transport industry needs to find a cleaner way of flying so that the environment is not polluted and the public's health is not compromised by toxic emissions such as nitrous oxides, NO_x, trioxygen, O_3, and particulate matter, $PM_{2.5}$ [1]. The European aviation sector is looking for ways to enhance aircraft operational performance and the environmental health of its aerospace industry. Aircraft emissions account for 2% of carbon emissions globally. The EU's aviation industry makes up for 3% of the overall greenhouse gas emissions. Studies show that if existing technology is not developed, emissions are likely to increase by two and half times due to the blossoming middle class in developing regions of the world such as Africa, China, India, and Brazil, where people increasingly want to travel. The first target is to replace 10% of fuel with low-carbon alternatives in the next ten years. And the second is to begin developing a carbon-free fuel from renewable energy sources [2]. This is a result of energy used for lift and drag. EU member nations were required to advance a national strategy to achieve a climate-neutral economy, in accordance with the Paris Agreement, by the year 2050.

The electrical systems are used to power avionics and lighting systems; the hydraulic system is used for most aircraft actuation systems, and the pneumatic system provides for loads such as pressurization of the cabin and air-conditioning. The mechanical system pumps the fuel and oil [3]. Over the years, aircraft manufacturers have increasingly replaced hydraulic and pneumatic systems with electrical systems to reduce fuel consumption and operating costs and minimize the environmental

http://doi.org/10.30684/etj.2022.133963.1214
Received 20 May 2022; Accepted 22 July 2022; Available online 28 September 2022
2412-0758/University of Technology-Iraq, Baghdad, Iraq

impact of flying. This approach to aircraft design is called the More Electric Aircraft Concept (MEA). The MEA concept relates to the non-propulsive systems of the aircraft. It is a trend that gradually began in 1967 with the introduction of the electric cabin and avionics to the Boeing 737 aircraft and has continued since [4]. The EAP concept requires rapid technological development as opposed to the MEA concept. The redesign of general aviation will not substantially affect overall CO_2 emissions in the aviation industry, so it is necessary to focus on single and twin-aisle aircraft and invent more powerful technologies to reduce carbon emissions. The Boeing SUGAR (Subsonic Ultra-Green Aircraft Research) concept is a sequence of aircraft designs issued by The National Aeronautic and Space Administration (NASA); these aircraft configurations were designed in the 2000s. Compared with current technology. The SUGAR Volt concept decreases carbon emissions by 70% [5]. The Navier-Stokes equations are a partial differential equations that accurately describe viscous fluids' behavior, modeled as a continuum rather than discrete particles. The Navier-Stokes equations are complex and unstable and do not have an exact solution, meaning "many solutions are generated that must be averaged to produce engineering quantities such as lift or drag from a pressure solution. [6].This calls for computational fluid Dynamics (CFD) in assessing powering turbofan propulsion passenger aircraft with electricity based on aircraft flying parameters.

The aeroplane uses LNG liquefied natural gas to produce electricity in flight and integrates a fuel cell with the turbine engine. “The aft propulsor in the aircraft is run with electrical energy to power the boundary layer and reduce drag” [7]. Actualizing this concept is still miles away as the technologies required for the concept's operation are still under development and are within the N+4 timeframe. The integration of the tanks and engines is a safety concern, and liquid natural gas produces methane emissions that are harmful to the environment. The advantage offered by a turboelectric propulsion system is the reduction in greenhouse gas emissions and noise pollution. Inside gas turbine engines, nitric oxide and nitrogen dioxide are generated. Aircraft exhaust emissions have a devastating effect on the environment. The N3-X configuration reduces nitrogen emissions and exceeds emissions standards by 85 percent [8].

Although this series of aircraft models have greatly benefited the aviation sector, it has failed to address the issue of environmental consequences and noise pollution. They have also failed to address an aircraft's high energy usage and high power requirement. These inadequacies give birth to the electrification of aircraft propulsion systems. In the early 2000s, aeronautical engineers began to think and analyze ways to electrify aircraft propulsion systems; the prototypes were designed and developed by NASA using various computer software. As observed from the existing knowledge, no one has used computational fluid dynamics (CFD) simulations to compare the influence of energy and power requirements of an electric turbofan aircraft at various stages of flight with that of the conventional turbofan aircraft to determine which is more aerodynamic. Hence assessment of powering turbofan propulsion passenger aircraft with electricity using CFD simulation was studied

2. Materials

The Reynolds-averaged Navier-Stokes (RANS) Simulation approach was used within Computational Fluid Dynamics (CFD) to simulate different engineering flows. The use of turbulence models (like k-omega & k-epsilon) helped to solve turbulence flows and measured turbulence-induced stress. The function of CFD within aircraft design was to characterize flow regimes in and around the aircraft detailing the shear stress, pressure, and flow velocities that the aircraft structure undergoes.

2.1 Method Used for the Simulation

The parameters affecting how the airflow behaves are density ρ, velocity v, length L, and kinematic viscosity μ. The airflow within the control volume followed the conservation laws of mass momentum and energy. Ansys Fluid Flow is used to analyze the airflow properties over the aircraft. Eq. 3 shows the Reynolds Number Equation.

$$Re = \frac{pvL}{\mu} \tag{1}$$

The first layer height is determined using Eq. 2 to 5 below [9]. “The cell wall distance parameter, or y+, which is a non-dimensional property, defines the distance between the wall and a given cell height as a function of the flow property [10].

$$C_f = (2log_{10}(Re_x) - 0.65)^{-2.3}\ for\ Re_x < 10^9 \tag{2}$$

$$\tau_w = C_f.\frac{1}{2}\rho {U_{freestream}}^2 \tag{3}$$

$$U_* = \sqrt{\frac{\tau_w}{\rho}} \tag{4}$$

$$y = \frac{y^+\mu}{\rho u_*} \tag{5}$$

Table 1 shows that the flow is fully turbulent. Therefore a turbulence model is needed to resolve the flow problem in the viscous sub-layer of the boundary region. There exist many turbulence models that can also be applied to model the flow within the boundary layer, but the model preferred for this simulation is the k-ω SST (Shear-Stress Transport).

Table 1: Wall distance according to flow conditions

Reynolds Number	Inlet velocity (m/s)	Mach Number	First Layer Height (y) When y+=1
$16.4x10^6$	20	0.068	$6.94x10^{-5}$ m
$41.1x10^6$	50	0.169	$2.96x10^{-5}$ m
$82.2x10^6$	100	0.339	$1.55x10^{-5}$ m
$143.9x10^6$	175	0.593	$9.19x10^{-6}$ m
$190.8x10^6$	232*	0.785	$7.06\ x10^{-6}$ m

* To the nearest 1 m/s

Eq. 6 shows the two equations that SST k-ω uses to capture the behavior of the viscous sublayer:

$$\frac{d}{dt}(pk) + \frac{d}{dx_i}(pkv_i) = \frac{d}{dx_j}\left(\Gamma_k \frac{dk}{d_j}\right) + \tilde{G}_k - Y_k + S_k$$

$$\frac{d}{dt}(p\omega) + \frac{d}{dx_i}(pwv_i) = \frac{d}{dx_j}\left(\Gamma_\omega \frac{d_\omega}{dx_j}\right) + \tilde{G}_\omega - Y_\omega + D_\omega + S_w \quad (6)$$

Where $Y_k$and $Y_\omega$are the dissipation of k and ω due to turbulence. G_k is the production of turbulence kinetic energy due to mean velocity gradients and G_ω is the production of ω.Γ_ω and Γ_k are the effective diffusivity of ω and k, respectively. D_ω Stands for cross-diffusion and S_k and S_ω are the optional sources in the model [11]

2.2 Comparison Between the Two Aircrafts Useful 300 Seat Case Payload Passenger Transporter

The case of 300 passengers in Figure 1 affected the observation below. The conceptual design of a 300-seat, wingspan-limited C-wing Figure 2. was examined. The results obtained with simple analytical and semi-empirical methods have been corroborated, in some validation computations, by those of more complex methods. The main findings of the design process and the subsequent analysis are summarized in the next statements. The medium size was flying wing configurations technically feasible and operationally efficient and could beat conventional airplanes of similar size. No infrastructure compatibility problems exist if the maximum span is kept below 80 m. The flying wing's main advantages are field and cruise performances, with take-off and landing field length values analogous to much smaller aircraft. The medium size flying wing is 10-20 percent more efficient as a transport vehicle than conventional airplanes, measured in terms of global transport productivity. The flying wing configuration may better exploit emerging technologies like LFC over a large fraction of the wetted area, composites and aeroelastic tailoring in primary structure, and ultra-high bypass ratio engines mounted over the wing. The main drawbacks of the C-wing configuration are the uncommon wing architecture, which may imply manufacturing and maintenance problems, uncommon cabin arrangement, which may be negatively perceived by passengers, and increased passenger and cargo flight loads for increased distance to the airplane axis, with Table 1 as flow conations velocity to nearest 1 m/s for the avoidance of error uncertainty

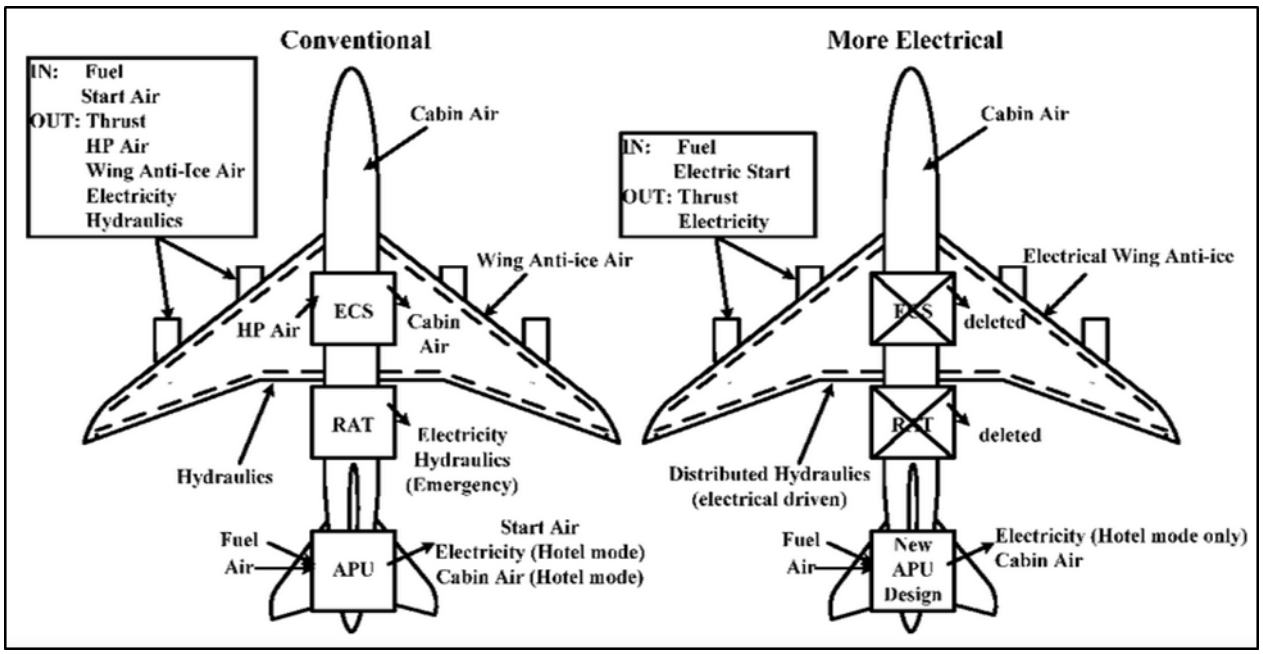

Figure 1: Comparison between the two aircraft useful 300 seat case payload passenger transporter

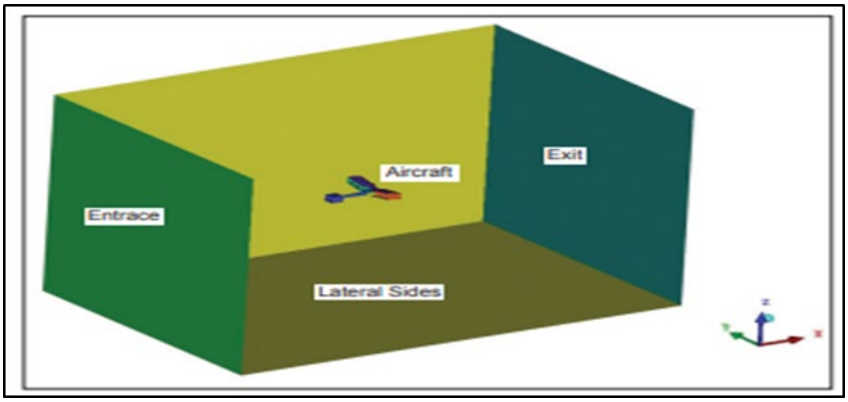

Figure 2: General overview of the computational domain

2.3 Boundary Conditions

The domain has 5 types of boundaries: the inlet, the outlet, the side walls, the aircraft model, and the symmetry wall. The air flows perpendicular to the inlet in a longitudinal direction parallel to the x-axis. There is a no-slip condition on the side walls and the model. This accurately measures the friction flows exerted on the model by the airflow. The computational domains' boundaries are specified within ANSYS FLUENT; the boundary conditions are defined as follows: Inlet: The velocity at the inlet of the domain is set at 20m/s and increased for each subsequent simulation until the final simulation is performed at 232 m/s. Outlet: The outlet pressure is set at 0 Pa. Side Walls: The M_∞ is changed in accordance with the inlet velocity. At 232 m/s the M_∞ is set at 0.785 for the side wall in the x-direction. Aircraft: The airplane model is considered a wall, and the roughness is the default. Symmetry Wall: The boundary condition for this wall is set to symmetry.

2.4 Description of Simulation Setup

In this work, a commercial code Computational Fluid Dynamics (CFD), is employed to perform the simulation. Several steps are carried out to get the result. In the first step, the model is developed using CAD software. Then, the model is imported to the computational domain. The computational domain is divided into a mesh. In the computational domain, the boundary values are imposed. A grid must be generated before the definition of physical properties, and boundary conditions are made. The accuracy of CFD depends on the quality of the grid and the number of cells in the domain. Finally, the governing equations and boundary values are solved iteratively using the CFD commercial code. Table 2 shows the design features of the Boeing 777-800 aircraft that are analyzed within ANSYS FLUENT [12].

Table 2: Design Parameters of Boeing 777-800 model aircraft [12]

Operating Conditions	**Details Plane**
h =12,496.8m	W_{plane} = 41145 kg
T_∞= 216 K	S = 125.0 m^2
p_∞= 0.296 kgm^{-3}	b = 34.31m
P_∞ = 18422.8 Pa	F_{engine} = 121400N
a =294.9 ms^{-1}	L = 39.5m
μ =1.422x10^{-5}Pa.s	v = 232ms^{-1}

2.5 Initial Properties

The airflow over the aircraft is simulated within ANSYS at different velocities. The air speeds over the aircraft are 20m/s, 50m/s, 100m/s, 175 m/s and 232m/s, respectively. The transonic airflow speeds simulated within ANSYS FLUENT can be compared to the cruise speed of a conventional aircraft and enables a realistic assessment of the power needed for an airplane to fly. The airflow is directed parallel to the x-axis and in the opposite direction of the nose of the aeroplane. A flow is considered incompressible when the M_∞≤0.3, the higher air speeds (100 m/s, 175m/s, 232 m/s) simulated within ANSYS FLUENT can be considered subsonic flow regimes. The flow problem is modeled as a subsonic compressible flow at cruise speed. Equ.3.7 shows the free stream Mach number (M_∞) at cruise speed.

$$M_\infty = \frac{v}{a} = \frac{232}{295} = 0.785 \quad (7)$$

There are two different discrete solvers, the pressure-based solvers, and the density-based solver. Each of the solvers makes use of control-volume methods.

2.6 Mesh Information

Meanwhile, the mesh size is coarse, and poor accurate result is imminent since no mesh size could exceed 20millions The mesh size is kept constant. Finally, the mesh structure is refined to optimize the accuracy of the solution generated. 20 Inflation layers were added to capture the turbulent flows around the boundary region with a growth rate of 1.2, Figure 3.

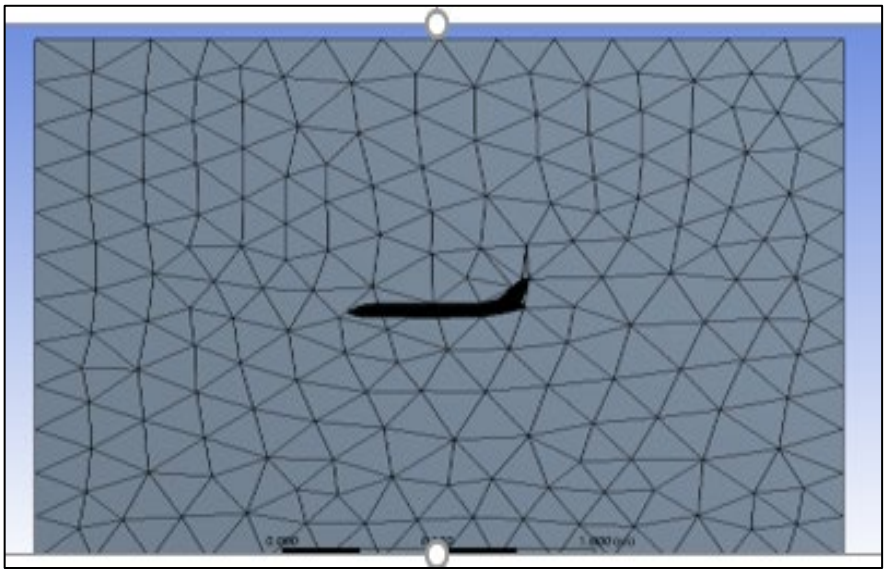

Figure 3: Mesh along the symmetry plane

3. Results and Discussion

Tables 3 and 4 show the mesh sizes for the analysis of the conventional aircraft and flying wing aircraft

Table 3: Lift and drag of conventional aircraft at different mesh sizes

Element Size (m)	Nodes	Elements	Lift (N)	Drag(N)
0.19	379473	934525	106060	-223870
0.17	476930	1197770	102460	-216780
0.14	716013	1872764	269110	-260940
0.13	842547	2235381	286920	-273330

Table 4: Lift and drag of flying wing aircraft at different mesh sizes

Element Size (m)	Nodes	Elements	Lift (N)	Drag(N)
0.19	264551	611593	10080	-7577
0.16	386193	909458	9940	-7591
0.14	510307	1224810	10662	-7677
0.12	702920	1730410	10124	-7650

The mesh was considered refined because the lift and drag values change approximately 18000N and 13000N across the two finest meshes within the specified tolerance of 10%. The difference between lift and drag values across the mesh size was around 1.39% and 1.30%, respectively. Therefore, the finest mesh was chosen and used to perform all simulations. Figures 4 and 5 show the independent mesh studies for both aircraft comparisons. It is evident from Figure 4 that in lift and drag of

conventional aircraft, lift increased as the node increased while the drag moved in the opposite direction to the movement of the lift. However, Figure 5 shows that in the Lift and drag of flying wing aircraft, the drag increased as the node increased, but the increase was not significant to counter the aircraft's thrust at cruise speed.

The endurance in Tables 3 and 4 are. Table 3 has endurance. (0.19+0.17+0.15+0.14)/4 = 0.1625. Table 4 has endurance, (0.19+0.116+0.14+0.12)/4 = 0.1525. Then endurance Table 3 and 4 is 0.01, which is 1 error reduction in endurance

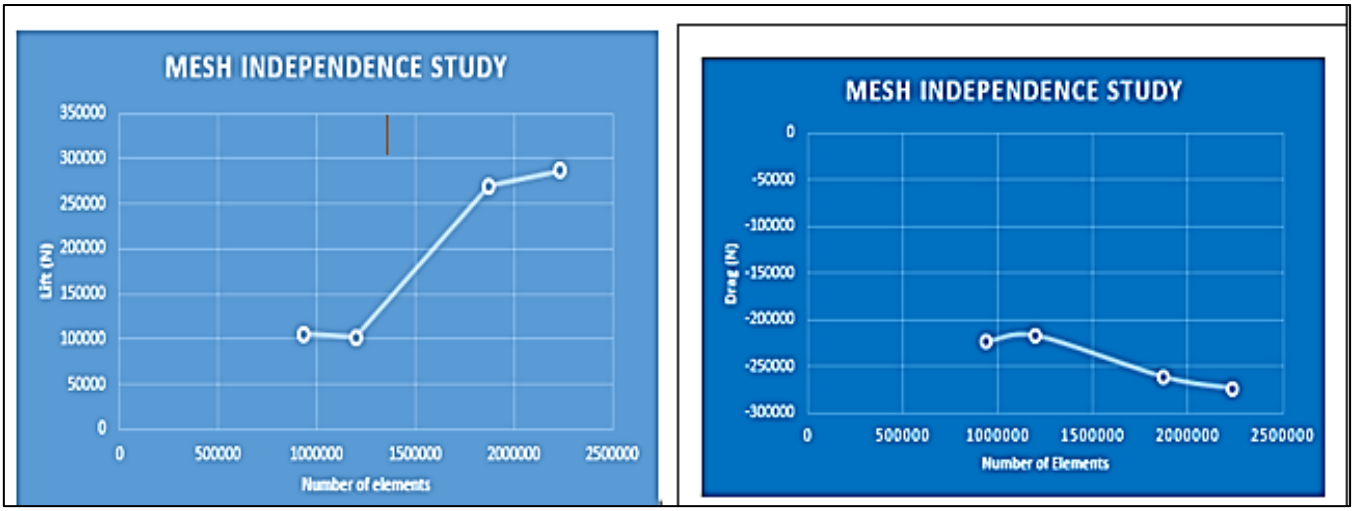

Figure 4: Lift and drag of conventional aircraft

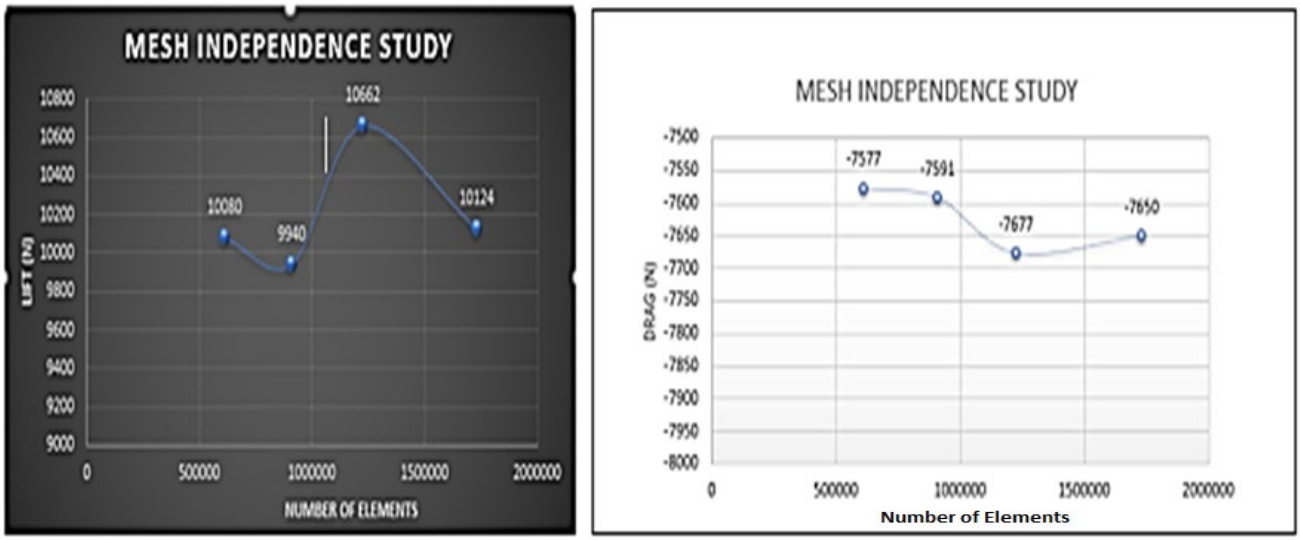

Figure 5: Lift and drag of electric flying wing aircraft

3.1 Pressure Contour

From Figure 6, the aircraft is moved within the green region. This showed that the conventional aircraft was cruising with moderate pressure due to the effect of the high drag. In contracts, Figure 7 aircraft was seen at a high pressure distributed along the fuselage and wing, overcoming the drag.

3.2 Velocity Contour

The velocity contour in Figure 8 shows high drag affecting the streamlined movement of the aircraft. The direction of the arrow shows that the drag could not allow the aeroplane to attend its cruise speed. However, the velocity contour in Figure 9 shows how the thrust overcame the drag, and the aircraft movement was smooth. Again, the direction of the arrow shows that the thrust was not much affected by the less drag.

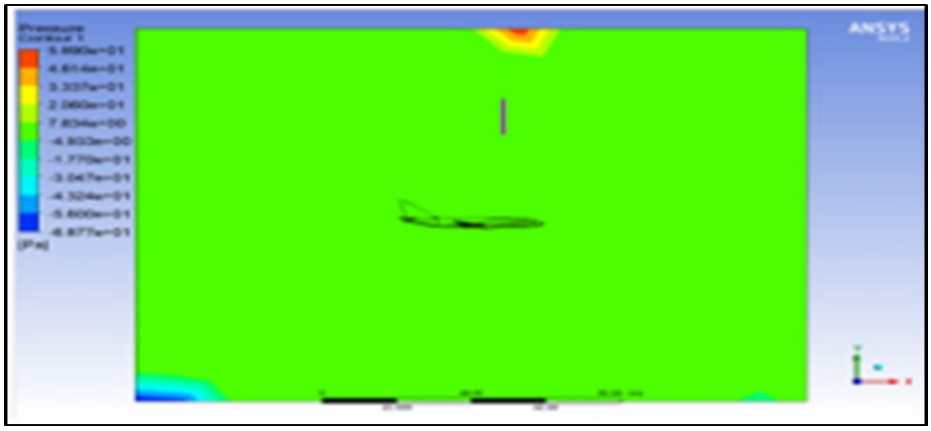

Figure 6: The pressure contours of conventional and Electric Aircraft

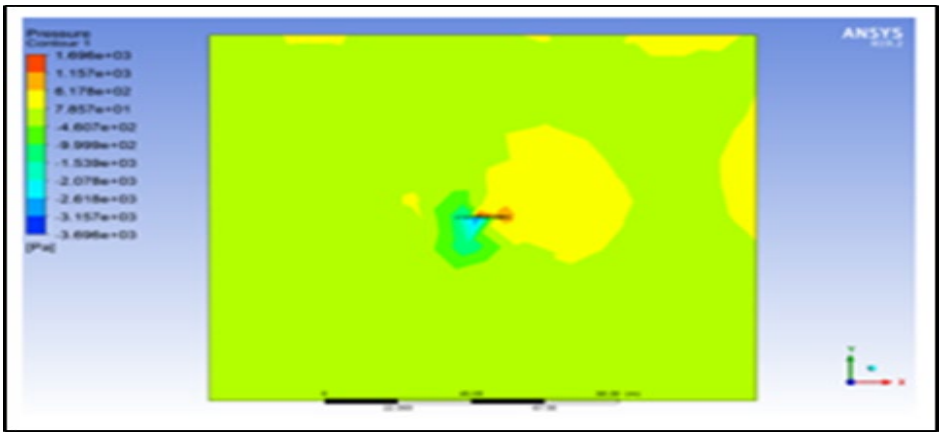

Figure 7: The pressure contours of conventional and Electric Aircraft

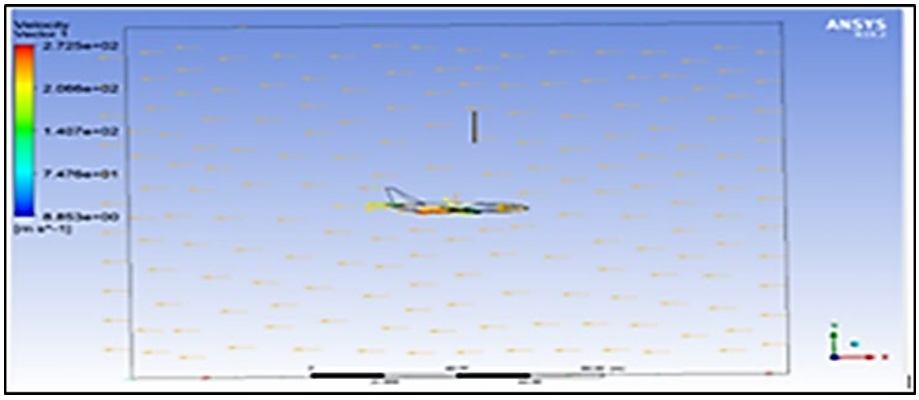

Figure 8: The velocity contours of conventional and Electric Aircraft

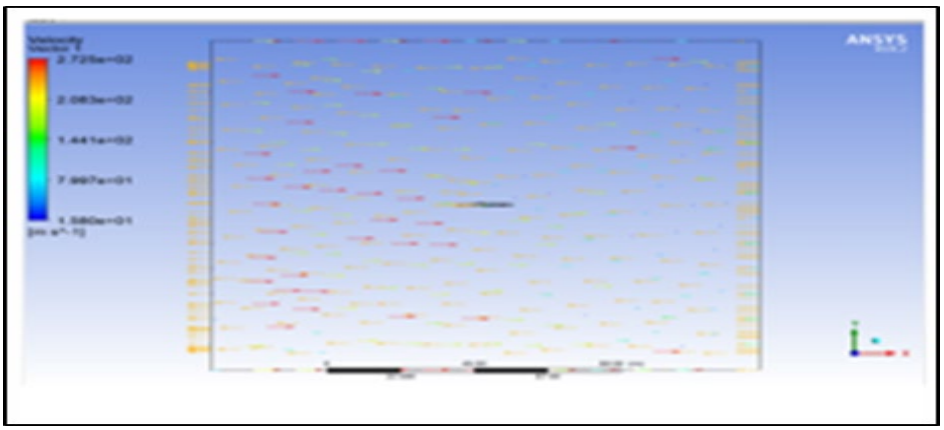

Figure 9: The velocity contours of conventional and Electric Aircraft

3.3 Power Requirements at Various Speeds

Tables 5 and 6 show the lift and drag for conventional and flying wing aircraft. Figure 9 illustrates the discrepancy between the power requirements of the two aircraft at several velocities. However, in Figures 10 and 11, the lift and drag of the conventional increased geometrically while the lift and drag of the electric flying wing aircraft (EFWA) increase linearly as the airspeed increases, which is not good for the aircraft performance. The lift at the cruise speed of the conventional aircraft is approximately 20 times larger than the FWA. Correspondingly, this lift at Mach 0.068 cruise speed of conventional aircraft is approximately 20 times heavier than FEA. Invariably, FWA is 95.37% more aerodynamically efficient than convectional aircraft.

Table 5: The lift and drag of the Boeing 737-800/900 at different velocities

Mach Number	Velocity (m/s)	Lift (N)	Drag (N)
0.068	20	109070	-4455
0.169	50	118030	-6412
0.339	100	138760	-48531
0.593	175	212850	-201270
0.785	232	269110	-260940

Table 6: The lift and drag of FWA at different velocities

Mach Number	Velocity (m/s)	Lift (N)	Drag (N)
0.068	20	5047	-7380
0.169	50	5221	-7396
0.339	100	5933	-7445
0.593	175	8732	-7553

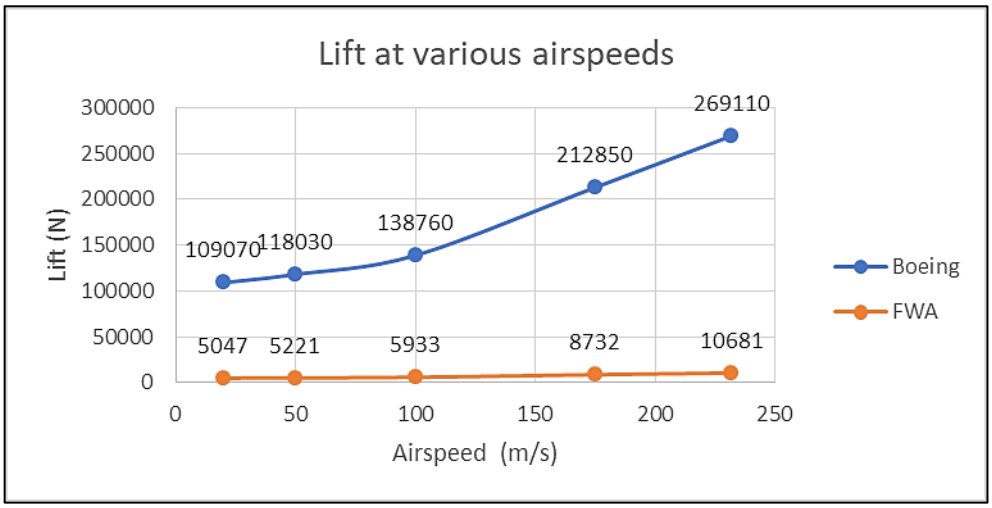

Figure 10: The lift and drag of conventional and Electric Aircraft

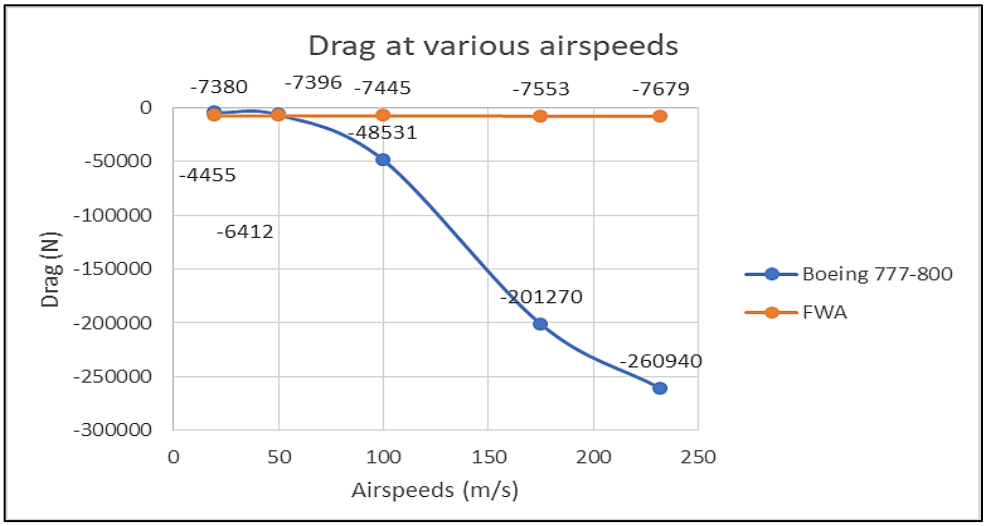

Figure 11: The lift and drag of conventional and Electric Aircraft

4. Conclusions

The assessment of powering turbofan propulsion passenger aircraft with electricity using computational fluid dynamics showed that less energy is used for a flying wing to fly at cruise speed than a conventional tube-and-wing aircraft. If less energy is used during the flight, less carbon emission would be emitted. The lift forces acting on the conventional aircraft and flying wing at cruise speed are 269,110 N and 10681 N, respectively. And the drag forces acting on the conventional aircraft and FWA at cruise speed are -260,940N and -7679N, respectively. A more realistic figure would be around -90,000N or the drag force acting on the flying wing. Either way, the indication is that the flying wing aircraft is more preferred than aerodynamic aircraft and uses less energy than the other aircraft when at cruise speed. Lastly, the more electric aircraft approach has allowed, the older power subsystems to be replaced by electrical systems within modern aircrafts such as the Boeing 777 and Airbus 380, which has increased fuel efficiency. All-electric aircraft greatly reduce fuel burn and emit no hazardous emissions. In electric configurations discussed within this thesis, the partial turboelectric configuration stands out as the best choice of a propulsion system for commercial aviation. The result of the lift power requirement obtained in this thesis should be a prerequisite for battery companies to develop FWA batteries

5. Further Works

1) Further assessments of different airframe configurations should be conducted so that the relative merits of each configuration can be ascertained. Finally, concepts like the Flying V, Strut Braced Wing, and the Cargo BWB should be developed and tested.
2) Many system studies have already been conducted concerning aircraft configurations and technology, but more studies need to comprehensively understand each concept's economic and environmental benefits.
3) Airlines should lobby governments for more funding so that research and development of existing concepts can occur and the carbon reduction goals can be achieved.
4) The aircraft lift and drag coefficients variation with the free stream velocity at variable aircraft angle of attack for zero wings incidence angle is recommended for further works
5) The CFD analysis on models rather than full-scale prototypes with the consideration of similarity requirements ought to be carried out

Author contribution

All authors contributed equally to this work.

Funding

This research received no specific grant from any funding agency in the public, commercial, or not-for-profit sectors.

Data availability statement

The data that support the findings of this study are available on request from the corresponding author.

Conflicts of interest

The authors declare that there is no conflict of interest.

References

[1] J. Domone, The challenges and benefits of the electrification of aircraft, SNC-Lavalin's Atkins, London, 2018.

[2] International Air Transport Association, IATA Calls for a Zero Emissions Future, 2007.

[3] P. Wheeler, S. Bozhko, The More Electric Aircraft: Technology and challenges, IEEE Electrif. Mag., 2 (2014) 6-12. https://doi.org/10.1109/MELE.2014.2360720

[4] R. Berger, Aircraft Electrical Propulsion –The Next Chapter of Aviation?, Think:Act, (2017) 1-32.

[5] B. Brelje, J. Martins, Electric, hybrid, and turboelectric fixed-wing aircraft: A review of concepts, models, and design approaches, Prog. Aerosp. Sci., 104 (2019) 1-19. https://doi.org/10.1016/j.paerosci.2018.06.004

[6] Symscape, Reynolds-Averaged Navier-Stokes Equations, 2009.

[7] NASA, Airplane Concepts, Glenn Research Center, 2017.

[8] H. D. Kim, J. L. Felder, M. T. Tong, Turboelectric distributed propulsion benefits on the N3-X vehicle, Aircr. Eng. Aerosp. Technol., 86 (2014) 558-561. https://doi.org/10.1108/AEAT-04-2014-0037

[9] CFD Online, Y plus wall distance estimation, CFD-Wiki, 2011.

[10] I. Rob, K. Stewart, B. Edet, H. Faik, Investigation of the Flow Around an Aircraft Wing of Section NACA 2412 Utilising ANSYS Fluent, INCAS BULLETIN, 10 (2018) 95-104. https://doi.org/10.13111/2066-8201.2018.10.1.10

[11] K. Lammers, Aerodynamic CFD analysis on experimental airplane, University of Twente & RMIT University, 2015.

[12] Airliners.Net, Boeing 737-800/900, VerticalScope Inc., 2002.